Journal of Physics: Condensed Matter

LETTER TO THE EDITOR

The phase transition sequence and the location of the morphotropic phase boundary region in $(1-x)[Pb(Mg_{1/3}Nb_{2/3})O_3]$–$xPbTiO_3$ single crystal

To cite this article: Yiping Guo *et al* 2003 *J. Phys.: Condens. Matter* **15** L77

INSTITUTE OF PHYSICS PUBLISHING JOURNAL OF PHYSICS: CONDENSED MATTER

J. Phys.: Condens. Matter **15** (2003) L77–L82 PII: S0953-8984(03)53429-4

LETTER TO THE EDITOR

The phase transition sequence and the location of the morphotropic phase boundary region in $(1-x)[Pb(Mg_{1/3}Nb_{2/3})O_3]$–$xPbTiO_3$ single crystal

Yiping Guo[1], **Haosu Luo, Di Ling, Haiqing Xu, Tianhou He and Zhiwen Yin**

State Key Laboratory of High Performance Ceramics and Superfine Microstructure, Shanghai Institute of Ceramics, Chinese Academy of Sciences, 215 Chengbei Road, Jiading, Shanghai 201800, China

E-mail: ggyp@sina.com

Received 13 September 2002
Published 6 January 2003
Online at stacks.iop.org/JPhysCM/15/L77

Abstract

Piezoelectric constant and temperature-dependent dielectric constant measurements have been performed on ⟨110⟩-oriented $(1-x)Pb(Mg_{1/3}Nb_{2/3})O_3$–$xPbTiO_3$ crystals with different compositions under different poling fields. The width of the morphotropic phase boundary region ($0.30 < x < 0.35$) is determined on the basis of two abnormal regions of the dielectric and piezoelectric properties. An irreversible rhombohedral–monoclinic M_A–monoclinic M_C–tetragonal phase transition sequence was observed directly from the dielectric constant versus temperature results for ⟨001⟩-poled rhombohedral crystals with compositions near the rhombohedral–monoclinic phase boundary. The structure of the morphotropic phase is shown to be monoclinic with space group P_m.

$(1-x)Pb(Mg_{1/3}Nb_{2/3})O_3$–$xPbTiO_3$ (PMN–PT) and $(1-x)Pb(Zn_{1/3}Nb_{2/3})O_3$–$xPbTiO_3$ (PZN–PT) single crystals, with compositions near their morphotropic phase boundaries (MPBs), have been reported to exhibit ultrahigh piezoelectric constants ($d_{33} > 2000$ pC N^{-1}), extremely large piezoelectric strains (>1.7%), and very high electromechanical coupling coefficients ($k_{33} > 92\%$) [1–5]. Recent experimental and theoretical studies have indicated that this strong piezoelectric response could be driven by polarization rotation induced by an external electric field in these single crystals [6, 7].

Despite these recent advances, many features related to phase transition behaviour in dielectric and piezoelectric properties of ferroelectric perovskite near the MPB remain puzzling. For instance, the experimental x-ray studies by Noheda *et al* [7] on ⟨001⟩-poled

[1] Author to whom any correspondence should be addressed.

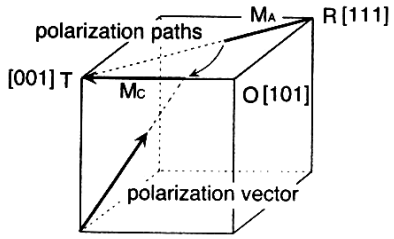

Figure 1. The polarization path for the PZN–8% PT crystal (see [7, 8]).

PZN–8% PT crystal suggests a complex rhombohedral (R)–monoclinic M_A–monoclinic M_C–tetragonal (T) phase transition sequence; i.e. the zero-field rhombohedral phase starts to follow the direct polarization path to tetragonal symmetry via an intermediate monoclinic M_A phase (space group C_m with the monoclinic b-axis along pseudocubic $[1\bar{1}0]$, and the polarization inside the $(1\bar{1}0)$ plane), but then jumps irreversibly to a monoclinic M_C phase (space group P_m with the monoclinic b-axis along pseudocubic [010], and the polarization inside the (010) plane). Recently, this irreversible R–M_A–M_C–T polarization path has been confirmed by neutron diffraction [8]. First-principles calculations by Bellaiche *et al* for the rhombohedral $Pb(Zr_xTi_{1-x})O_3$ (PZT) system under a $\langle 001 \rangle$ field also predict the R–M_A–M_C–T transformation, but applying an electric field of $\langle 111 \rangle$ orientation to tetragonal PZT leads to the expected T–M_A–R phase transition sequence [9]. Figure 1 depicts the path followed by the polarization rotation for the R–M_A–M_C–T phase transition sequence proposed. Furthermore, evidence of a monoclinic M_C phase in unpoled PMN–35% PT and PZN–9% PT crystals has been proposed by Kiat *et al* from a neutron Rietveld analysis [10], which is different from that proposed by Ye *et al* [11]. Very recently, a metastable orthorhombic ferroelectric (FE_o) phase and high piezoelectric coefficients ($d_{33} \sim 1600$ pC N^{-1}) have also been found for $\langle 110 \rangle$-oriented PMN–PT and PZN–PT single crystals near their MPBs [12–15]. However, there are still some questions currently unanswered. If there is indeed a new R–M_A–M_C–T transformation in PZN–PT, PZT, and even PMN–PT, can it observed directly from the measurements of dielectric and piezoelectric properties of $\langle 001 \rangle$-poled crystals? Why does the greatest piezoelectricity appear in the rhombohedral phase near the MPB?

In the present work, we address the problems summarized above by investigating the effect of composition and poling field on the dielectric and piezoelectric properties of PMN–PT crystals. The width of the morphotropic phase boundary region at room temperature is determined on the basis of two abnormal regions of the dielectric and piezoelectric properties for $\langle 110 \rangle$-oriented crystals. We also find that applying an electric field along the $\langle 001 \rangle$ pseudocubic direction for crystals with composition near the rhombohedral–monoclinic phase boundary does not simply generate the reverse transition sequence R–M_A–T. Instead, an irreversible R–M_A–M_C–T transition sequence is found.

The PMN–PT single crystals were grown directly from the melt by a modified Bridgman technique, in which $\langle 110 \rangle$-oriented seed crystals were used. The details have been described elsewhere [16]. It was reported that the segregation behaviour during the growth resulted in a variation of $PbTiO_3$ (PT) along the longitudinal direction of a boule. The Curie temperature (T_C) of PMN–PT was sensitive to the content of PT, so the content of PT in the samples was determined by measurement of the Curie temperature T_C in our experiments. The samples with different PT contents were poled in silicon oil with different fields (from 2 to 30 kV cm^{-1}) at room temperature. Dielectric constant measurements as a function of temperature were measured by using a HP4192A impedance analyser. The piezoelectric

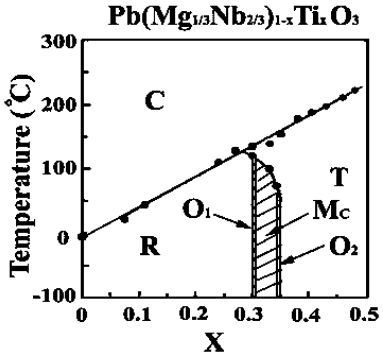

Figure 2. The phase diagram of the PMN–PT solid-solution system. Solid circles and related phase boundaries are adapted from [17], C, R, T, M, and O refer to cubic, rhombohedral, tetragonal, monoclinic, and orthorhombic phase regions, respectively. The diagonally shaded area has been updated on the basis of the present work.

constant (d_{33}) was measured by using a Berlincourt-type quasistatic meter at about 55 Hz. The domain configuration was observed using a crossed Olympus prism under a polarization microscope. The modified phase diagram of PMN–PT is shown in figure 2, on the basis of the phase transition behaviour and ferroelectric-related properties for crystals with different PT contents.

Figures 3(a)–(f) show the dielectric constant as a function of temperature and poling field for ⟨110⟩-oriented crystals. For PMN–29.5% PT crystal in the 'R' composition region (even PMN–29% PT), two small peaks of the dielectric constant R $\rightarrow$ O and O $\rightarrow$ T phase transitions are always observed even with a high poling field (30 kV cm^{-1}) (figure 3(a)), and a strong piezoelectric response $d_{33} \sim 1500$ pC N^{-1} can be always obtained, which is almost independent of the poling field. For PMN–30% PT crystal in the 'O_1' composition region, a small poling field lower than 3–4 kV cm^{-1} can induce a polydomain R (or M_A) and O state; two small peaks of the dielectric constant R $\rightarrow$ O and O $\rightarrow$ T phase transitions are observed (figure 3(b)). But a poling field higher than 4–5 kV cm^{-1} can induce a monodomain O state, as has been confirmed through the *in situ* observation of the ferroelectric domain configuration under polarization microscopes in the previous works [14, 15]; only one small peak of the dielectric constant is observed (figure 3(b)), which indicates a transition from the O to the T phase. The piezoelectric coefficients $d_{33} \sim 1600$ pC N^{-1} for a polydomain state and $d_{33} \sim 300$ pC N^{-1} for a monodomain state are found. For crystals in the 'M_C' composition region ($0.30 < x < 0.35$), one small peak of the dielectric constant (figures 3(c), (d)) and a weak piezoelectric response ($d_{33} \sim 300$ pC N^{-1}), which is independent of the poling field, should be attributed to a recovered M state, according to the results of *in situ* domain observation [14]. For PMN–35% PT crystal in another narrow 'O_2' composition region, a small poling field lower than 4–5 kV cm^{-1} can induce a polydomain T and O state; the abnormally high dielectric constant at room temperature implies that the phase transition O $\rightarrow$ T may occur below room temperature or under a higher poling field. Certainly, a poling field higher than 5–6 kV cm^{-1} can induce a monodomain O state; an abnormal point of the dielectric constant (O $\rightarrow$ T phase transition) is observed at 38 °C (figure 3(e)). The piezoelectric coefficients $d_{33} \sim 1500$ pC N^{-1} for a polydomain state and $d_{33} \sim 300$ pC N^{-1} for a monodomain state are found. This demonstrates that the field-induced orthorhombic ferroelectric phase was stable in this composition region at room temperature. For PMN–38% PT crystal in the 'T'

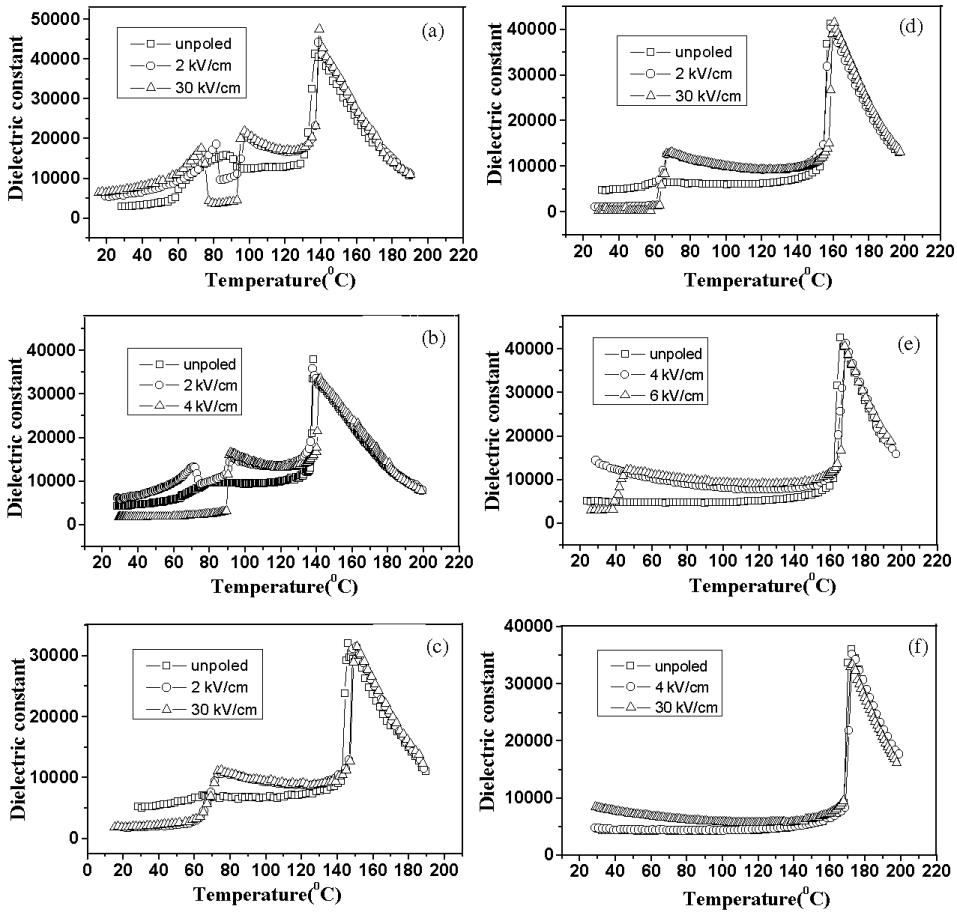

Figure 3. The dielectric constant as a function of temperature and poling field for ⟨110⟩-oriented PMN–PT crystals (1 kHz): (a) for PMN–29.5% PT crystal in the 'R' composition region, (b) for PMN–30% PT crystal in the narrow 'O_1' composition region, (c) for PMN–31% PT crystal in the 'M_C' composition region, (d) for PMN–34% PT crystal in the 'M_C' composition region, (e) for PMN–35% PT crystal in the 'O_2' composition region, (f) for PMN–37% PT crystal in the 'T' composition region.

composition region, a strong piezoelectric response ($d_{33} \sim 1300$ pC N^{-1}) at room temperature and an orthorhombic-to-tetragonal phase transition below room temperature have also been found [18]. Figure 3(f) shows the dielectric constant as a function of temperature and poling field from room temperature to 200 °C for PMN–37% PT crystal.

Figure 4 shows the dielectric constant as a function of temperature and poling field for ⟨001⟩-oriented PMN–30% PT crystal in the 'O_1' composition region. Two small dielectric peaks are observed even with a relatively low poling field (4 kV cm^{-1}), and a sharply enhanced piezoelectric constant is found due to enhanced polarization rotation: d_{33}1550 pC N^{-1} for the poled sample with $E_{poling} = 10$ kV cm^{-1}, and $d_{33} \sim 2500$ pC N^{-1} for the poled sample with $E_{poling} = 30$ kV cm^{-1}.

Piezoelectric coefficients d_{33} as a function of crystal composition and orientation for PMN–PT single crystals are shown in figure 5. Two abnormal points (or rather, almost certainly two narrow regions) of the piezoelectric constant appear clearly for ⟨110⟩-oriented crystals;

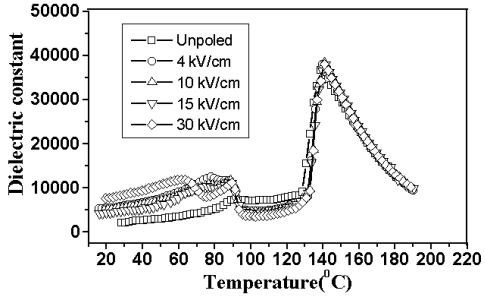

Figure 4. The dielectric constant as a function of temperature and poling field for ⟨001⟩-oriented PMN–30% PT crystal (1 kHz) in the narrow 'O_1' composition region.

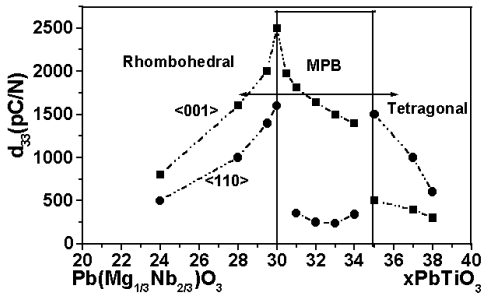

Figure 5. Piezoelectric coefficients d_{33} as a function of crystal composition and orientation for PMN–PT single crystals.

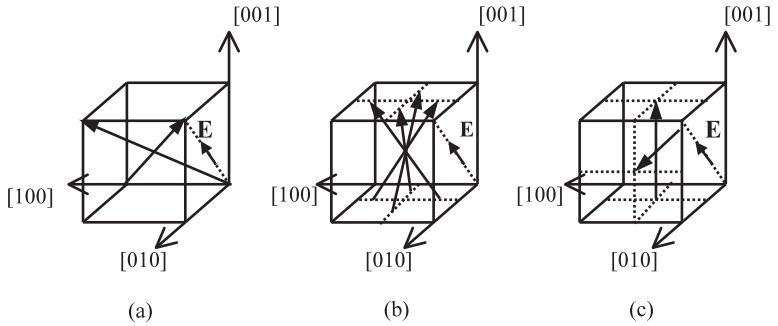

Figure 6. Schematic diagrams of possible polarization directions of domains for ⟨110⟩-poled crystals in different composition regions: (a) for crystals in the 'R' composition region; (b) for crystals in the 'M_C' composition region; (c) for crystals in the 'T' composition region.

the piezoelectric coefficients for the composition region $0.30 < x < 0.35$ are very low. It is known that the equivalent domain configuration is indispensable for a strong piezoelectric response in ferroelectric perovskite crystals. Figure 6 shows a schematic domain configuration for [101]-poled rhombohedral $3m$, monoclinic P_m, and tetragonal $4mm$ crystals. Therefore, the weak piezoelectric response for crystals in the 'M' composition region should be attributed to the nonequivalent domain configuration for ⟨110⟩-poled crystals. Thus the MPB composition region, separating the tetragonal ($x \geqslant 0.35$) and rhombohedral ($x \leqslant 0.30$) phase fields, should lie in the composition range $0.30 < x < 0.35$. The width of the MPB region in our samples is in perfect accord with that reported by Singh *et al* [19].

It is well known that the largest piezoelectric coefficients appear in the rhombohedral phase near MPB. But the mechanism underlying this ultrastrong piezoelectric response is not clear. The dielectric and piezoelectric behaviours for ⟨001⟩-oriented crystals with compositions near the rhombohedral–monoclinic phase boundary provide the first direct evidence for the origin of the very strong piezoelectricity. It is evident that a M_C monoclinic phase is induced when an electric field is applied along the ⟨001⟩ direction, and the phase transformation sequence between the rhombohedral phase and tetragonal phase should be similar to that of PZN–8% PT [7, 8], i.e., the irreversible R–M_A–M_C–T phase transformation sequence; the sharply enhanced piezoelectric response should be attributed to the polarization rotation from the M_A to the M_C phase. When the field is decreased to zero, an O phase is reached, which can be viewed as an M_C phase with lattice parameters $a_m = c_m$. So the first small peak in figure 4, which is more dependent on the poling field, should indicate a transition from R (or M_A) to the O phase, and the second peak should indicate a transition from the O to the T phase. The structure of the morphotropic phase is shown to be monoclinic with space group P_m.

In conclusion, we propose that two-phase boundaries, i.e. rhombohedral–monoclinic and monoclinic–tetragonal boundaries, exist in the unpoled PMN–PT phase diagram, which establish the 'O_1' (PMN–30% PT) and 'O_2' (PMN–35% PT) composition regions as the end-members of the monoclinic phase of space group P_m. An ultrastrong piezoelectricity for ⟨001⟩-poled crystals with compositions near the rhombohedral–monoclinic phase boundary should be attributed to the irreversible polarization rotation from the M_A to the M_C phase.

This work was supported by the National Science Foundation of China (Grant No 59995520) and National 863 High Technology Foundation of China (Grant No 2002AA325130)

References

[1] Kuwata J, Uchino K and Nomura S 1981 *Ferroelectrics* **37** 579
[2] Kuwata J, Uchino K and Nomura S 1982 *Japan. J. Appl. Phys.* **21** 1298
[3] Harada K, Shimanuki S, Kobayashi T, Saitoh S and Yamashita Y 1998 *J. Am. Ceram. Soc.* **81** 2785
[4] Park S-E and Shrout T R 1997 *IEEE Trans. Ultrason. Ferroelectr. Freq. Control* **44** 1140
[5] Park S-E and Shrout T R 1997 *J. Appl. Phys.* **82** 1804
[6] Fu H and Cohen R E 2000 *Nature* **403** 281
[7] Noheda B, Cox D E, Shirane G, Park S-E, Cross L E and Zhong Z 2001 *Phys. Rev. Lett.* **86** 3891
[8] Ohwada K, Hirota K, Rehrig P W, Gehring P M, Noheda B, Fujii Y, Park S-E and Shirane G 2001 *J. Phys. Soc. Japan* **70** 2778
[9] Bellaiche L, Garcia A and Vanderbilt D 2001 *Phys. Rev.* B **64** 060103
[10] Kiat J-M, Uesu Y, Dkhil B, Matsuda M, Malibert C and Calvarin G 2002 *Phys. Rev.* B **65** 064106
[11] Ye Z-G, Noheda B, Dong M, Cox D E and Shirane G 2001 *Phys. Rev.* B **64** 184114
[12] Lu Y, Jeong D-Y, Cheng Z-Y and Zhang Q M 2001 *Appl. Phys. Lett.* **78** 3109
[13] Viehland D 2000 *J. Appl. Phys.* **88** 4794
[14] Guo Y, Luo H, He T, Xu H and Yin Z 2002 *Japan. J. Appl. Phys.* **41** 1451
[15] Guo Y, Luo H, Xu H, Wang P and Yin Z 2002 *Ferroelectrics* **281** 93
[16] Luo H, Xu G, Wang P, Xu H and Yin Z 2000 *Japan. J. Appl. Phys.* **39** 5581
[17] Shrout T R, Chang Z P, Kim N and Markgraf S 1990 *Ferroelectr. Lett.* **12** 63
[18] Cao H *et al Japan. J. Appl. Phys.* submitted
[19] Singh A K and Pandey D 2001 *J. Phys.: Condens. Matter* **13** L931